

Evaluation of the complex atomic susceptibility of $\text{Er}^{3+}:\text{Ti}:\text{LiNbO}_3$ optical waveguides in visible and near IR spectral range

N. N. PUȘCAȘ

University "Politehnica" Bucharest, Physics Department, Splaiul Independentei, 313, 060042, Bucharest, Romania

Based on the transmission and emission experimental spectra of Er^{3+} -doped $\text{Ti}:\text{LiNbO}_3$ optical waveguides in this paper we report some experimental and theoretical results concerning the evaluation of the real and imaginary parts of the complex atomic susceptibility of the above mentioned waveguides in the visible and near IR spectral range. The absorption and emission experimental spectra were used to determine the homogeneous absorption and emission cross sections (utilising the density matrix formalism and the McCumber's theory and taking into account the Stark splitting of the levels) around 1550 nm, 980 nm and 550 nm, respectively and finally for the evaluation of the complex atomic susceptibility.

(Received May 08, 2009; accepted October 29, 2009)

Keywords: Er^{3+} -doped $\text{Ti}:\text{LiNbO}_3$ optical waveguides, Absorption and emission cross sections, Atomic susceptibility

1. Introduction

The absorption and emission cross sections of Er^{3+} -doped $\text{Ti}:\text{LiNbO}_3$ optical waveguides are widely used for the theoretical modelling of the guided lasers and amplifiers, design of complex integrated optoelectronic circuits etc., the exact knowledge of them playing a very important role [1-5].

Using the obtained transmission and emission experimental spectra in the case of Er^{3+} -doped $\text{Ti}:\text{LiNbO}_3$ optical waveguides, in this paper we report an exact evaluation of the homogeneous absorption and emission cross-sections in three regions of the optical spectra: around 1550 nm, 980 nm and 550 nm, respectively. For the evaluation of the homogeneous absorption and emission cross-sections from the inhomogeneous ones, obtained experimentally we used the density matrix formalism and the McCumber's theory taking into account the Stark splitting of the levels [6-9]. Finally we used the homogeneous absorption and emission cross-sections for the evaluation of the real and imaginary parts of the complex atomic susceptibility.

The paper is organised as follows. In Section 2, we present the basic equations used for the evaluation of the real and imaginary parts of the complex atomic susceptibility of the above mentioned waveguides in the visible and near IR spectral range. Section 3 is dedicated to the discussion of the obtained results while in Sections 4 the conclusions of this work are outlined.

2. Theory

For the evaluation of the homogeneous absorption and emission cross-sections the interaction between the atomic system and the electric field may be described considering a three-level system Stark splitted and the semiclassical formalism presented in papers [6-8].

Based on the model presented in paper [6] the spectral real, $\chi'(\omega)$ and imaginary, $\chi''(\omega)$ parts of the complex atomic susceptibility,

$$\chi(\omega) = \chi'(\omega) + i\chi''(\omega) \quad (1)$$

may be evaluated using the equations:

$$\chi'(\omega) = -2n\varphi \sum_{jk} \frac{\sigma_{kj}(\omega) \omega_{kj} - \omega}{\omega_{kj} \Delta\omega_{kj}} \times \frac{P_e^H(\omega_p) + \sigma_a^H(\omega_p) \left[p_{2k} - p_{1j} + S \left[p_{2k} \sigma_a^H(\omega_s) - p_{1j} \sigma_e^H(\omega_s) \right] \tau \right]}{1 + \left[P_e^H(\omega_p) + \sigma_a^H(\omega_p) \right] + \left[S \left[\sigma_e^H(\omega_s) + \sigma_a^H(\omega_s) \right] \right] \tau} \quad (2)$$

and

$$\chi''(\omega) = \frac{n\varphi}{2\pi\nu} \frac{1}{1 + \left[P_e^H(\omega_p) + \sigma_a^H(\omega_p) \right] + \left[S \left[\sigma_e^H(\omega_s) + \sigma_a^H(\omega_s) \right] \right] \tau} \times \left\{ -\sigma_a(\omega) + P_e^H(\omega) \left[\sigma_e^H(\omega_p) - \sigma_a^H(\omega) \sigma_e^H(\omega_p) \right] \tau + S \left[\sigma_e^H(\omega) \sigma_a^H(\omega_s) - \sigma_a^H(\omega) \sigma_e^H(\omega_s) \right] \tau \right\} \quad (3)$$

$$\text{In Eqs. (2)-(3)} \quad P = \frac{P_p}{h\tilde{\nu}A_p}, \quad S = \frac{P_s}{h\tilde{\nu}A_s}, \quad \sigma_{a,e}^H(\omega_{p,s})$$

represent the homogeneous absorption, a and emission, e cross sections at the pump, p and signal (saturated), s frequencies, respectively having $P_{p,s}$ and $A_{p,s}$ powers and effective areas,

$$\sigma_{kj}(\omega) = \frac{1}{1 + 4 \left(\frac{\omega - \omega_{kj}}{\Delta\omega_{kj}} \right)^2} \frac{\lambda_{kj}^2}{2\pi n^2 \tau_{kj} \Delta\omega_{kj}} \quad (4)$$

is the cross section of Lorentzian line shape associated with the individual laser transition (jk) characterized by the wavelength λ_{kj} , linewidth, $\Delta\omega_{kj}$ and radiative lifetime, τ , n is the refractive index, ρ is the dopant ionic density and $\tilde{\nu}$ is an average frequency arbitrarily taken as any value of λ_{kj} which varies by only 1 % over the wavelength range of interest.

In Eq. (2) p_{nm} define the Boltzmann distribution of the populations, \bar{N}_n corresponding to individual Stark sublevels (Fig. 1):

$$N_{nm} = \frac{\exp\{-(E_m - E_n)/k_B T\}}{\sum_{m=1}^{\infty} \exp\{-(E_m - E_1)/k_B T\}} \tilde{N}_n = p_{nm} \tilde{N}_n, \quad (5)$$

$E_{1,2,3}$ being the energies of the levels and $g_{1,2,3}$ the degeneracies.

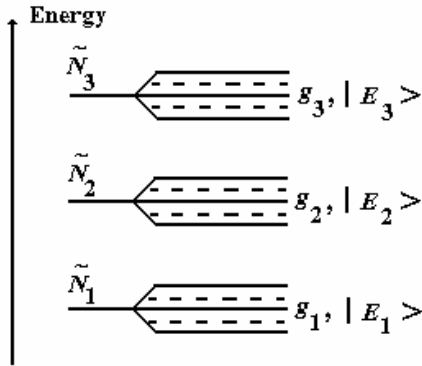


Fig. 1. The energy diagram corresponding to the Er^{3+} Stark split three-level system.

The effective areas, $A_{p,s}$ (Eqs. (2) and (3)) were evaluated from the fields profiles measured experimentally using the near field method in the case of the radiations around 1550 nm [5] and simulated for 980 nm and 550 nm, respectively using the formula:

$$A_{p,s} = \frac{\pi}{4} w_{p,s3} (w_{p,s1} + w_{p,s2}) \quad (6)$$

where $w_{p,s}$ are the parameters which characterize the mode profiles of the waveguide (Fig. 2).

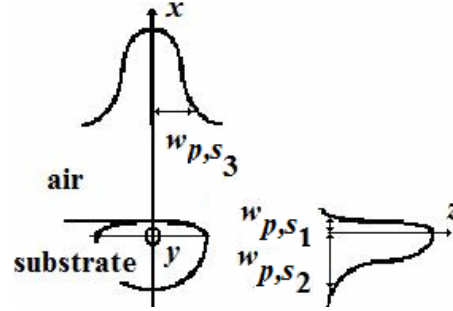


Fig. 2. The parameters which characterize the mode profiles in width and depth of the waveguide.

The homogeneous absorption and emission cross sections, $\sigma_{a,e}^H(\omega)$ may be determined from the experimental (inhomogeneous) cross sections $\sigma_{a,e}^I(\lambda)$ through the inverse Fourier transform relation (and its properties) [6]:

$$\sigma_{a,e}^H(\omega) = F^{-1} \left[\exp \left(\frac{\Delta\omega_{inh}^2 x^2}{16 \log 2} F[\sigma_a^I(\omega); x] \right) \right] \quad (7)$$

where $\Delta\omega = 2\pi c \Delta\lambda_{inh} / \lambda^2$ is the inhomogeneous bandwidth and $\Delta\lambda_{inh}$ the inhomogeneous linewidth. The relation between the absorption and emission cross sections is [6]:

$$\sigma_{a,e}^H(\omega) = F^{-1} \left[\exp \left(\frac{\Delta\omega_{inh}^2 x^2}{16 \log 2} F[\sigma_a^I(\omega); x] \right) \right] \quad (8)$$

where: T is the temperature, k_B is the Boltzmann's constant and \mathcal{E} represents the excitation energy.

The spectra can be numerically generated through the fitting formula [5], [6]:

$$I(\lambda) = \sum_i a_i \exp \left\{ -4 \log 2 [(\lambda - \lambda_i) / \Delta\lambda_i]^2 \right\}. \quad (9)$$

The experimental line shapes $I_{a,e}(\lambda) \approx \sigma_{a,e}^I(\lambda)$. The fitting curve is not unique but the deconvolution expressed in $\sigma_{a,e}^H(\omega)$ has a unique solution.

Knowing the emission cross section one can evaluate the radiative life time, τ using the following relation [6], [9]:

$$\frac{1}{\tau} = \frac{8\pi n^2}{c^2} \int v^2 \sigma_e(v) dv. \quad (10)$$

3. Discussion of the results

Using the experimental setup presented in papers [5], [8] and [9] we measured at room temperature the nonpolarised absorption spectra around: 1530 nm (corresponding to the transition ${}^4I_{15/2} \rightarrow {}^4I_{13/2}$), 980 nm (corresponding to the transition ${}^4I_{15/2} \rightarrow {}^4I_{11/2}$) and 550 nm (corresponding to the transition ${}^4I_{15/2} \rightarrow {}^4S_{3/2}$) of a 7.5 μm $\text{Er}^{3+}:\text{Ti}:\text{LiNbO}_3$ waveguide.

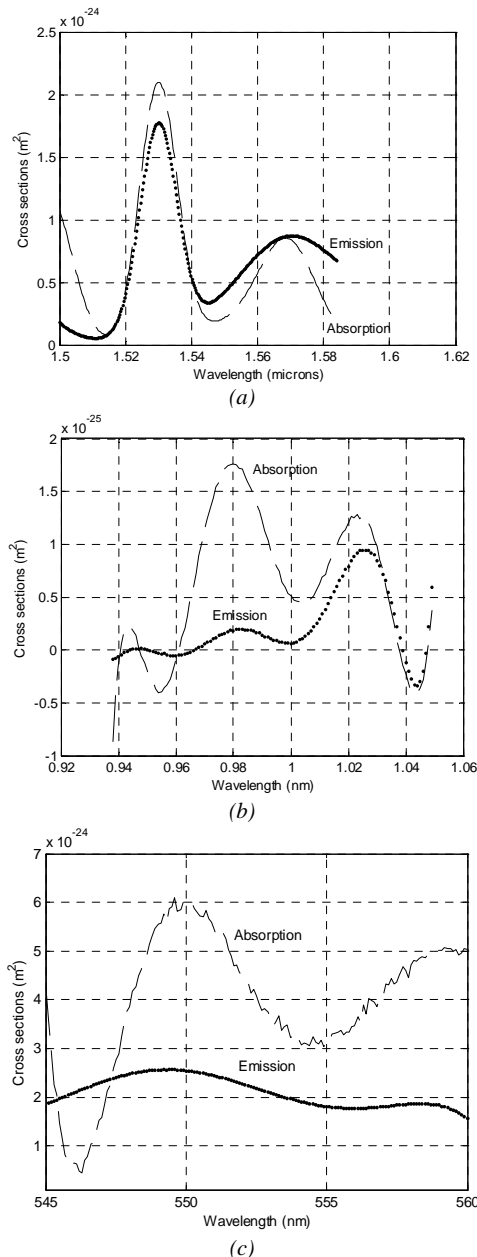


Fig. 3. The nonpolarised measured absorption spectra around: (a) 1530 nm, (b) 980 nm and (c) 550 nm.

Based on the theory presented in Section 2 of this article we evaluated the homogenous absorption and emission spectra (Fig. 3 (a), (b), (c)). For the simulation of the inhomogenous absorption spectra we used eight Gaussian functions to assure the best fit with the experimental data. The peak values of the evaluated the homogenous absorption and emission spectra and the radiative lifetimes corresponding to the above mentioned transitions are presented in Table 1. For the evaluation of the real and imaginary parts of the complex atomic susceptibility (Eqs. (2) and (3)) the refractive indices for several wavelengths were calculate using the Sellmeier equation. Also, we considered $\rho = 10^{25} \text{ m}^{-3}$ (widely used in the doping process) and we used the values of other spectroscopic parameters presented in paper [9].

The spectral dependence of the real and imaginary parts of the complex atomic susceptibility corresponding to the above mentioned transitions are presented in Figs. 4 (a), (b) and (c) and the peak values of the real part of the susceptibility are outlined in Table 1.

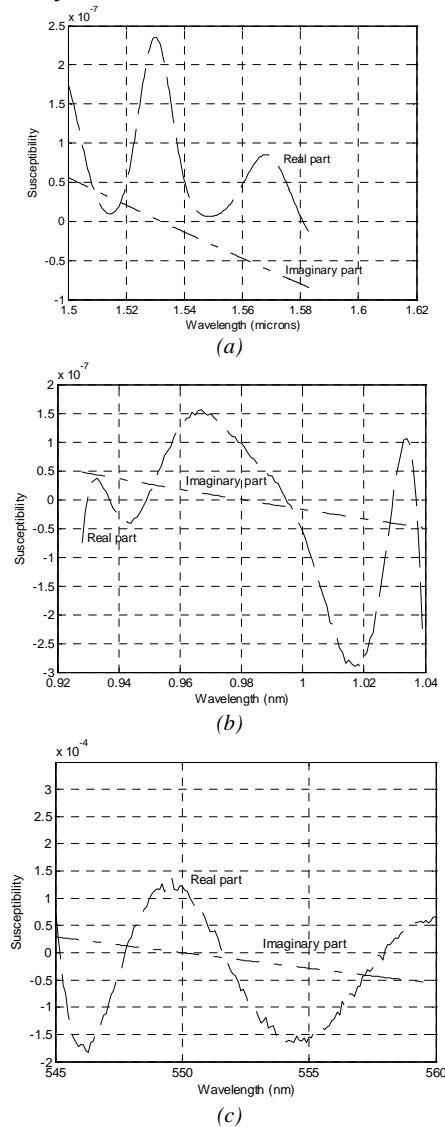


Fig. 4. The real and imaginary parts of the complex atomic susceptibility around: (a) 1530 nm, (b) 980 nm and (c) 550 nm.

As can be seen from Fig. 1 (a)-(c) the dependences of real part of the complex atomic susceptibility are determined by the homogeneous absorption and emission cross-sections while imaginary parts vary linear in the range of interest and vanish for the wavelength of the laser signal transitions. Also, the powers of the pump (more significant) and signal (less significant) radiations and the corresponding effective areas determine the values of the susceptibilities.

Table 1.

Parameter	$\lambda = 1530$ (nm)	$\lambda = 980$ (nm)	$\lambda = 550$ (nm)
$\sigma_a^H (\text{m}^2)$ $\times 10^{-24}$	0.13	0.76	1.32
$\sigma_e^H (\text{m}^2)$ $\times 10^{-24}$	0.18	0.65	0.58
$\tau(\text{s})$ (ms)	4.46	2.01	1.51
χ''	$2.4 \cdot 10^{-7}$	$9.7 \cdot 10^{-8}$	$1.2 \cdot 10^{-4}$

The real and imaginary parts of the complex atomic susceptibility are related to the power gain and gain-induced refractive index change [6].

4. Conclusions

In this paper we report some experimental and theoretical results concerning the evaluation of the real and imaginary parts of the complex atomic susceptibility of the Er^{3+} -doped Ti:LiNbO_3 optical waveguides in the visible and near IR spectral range.

For the spectral dependence of the susceptibilities (around 1550 nm, 980 nm and 550 nm, respectively) we

used the homogeneous absorption and emission cross sections evaluated according to the McCumber's theory and the density matrix formalism and taking into account the Stark splitting of the levels.

The dependences of real part of the complex atomic susceptibility are determined by the homogeneous absorption and emission cross-sections while imaginary parts vary linear in the range of interest vanishing for the wavelength of the laser signal transitions.

References

- [1] W. Sohler, H. Hu, R. Ricken, V. Quiring, C. Vannahme, H. Herrmann, D. Büchter, S. Reza, W. Grundkötter, S. Orlov, H. Suche, R. Nouroozi, Y. Min, ECIO'08, Optics & Photonics News, 24, 2008.
- [2] J. M. M. de Almeida, A. M. P. Leite, J. Amin. SPIE, **3942**, 232 (2000).
- [3] W. Sohler, Waveguide Optoelectronics, J. Marsh and R. de la Rue (eds.), NATO ASI Series E: Applied Sciences, Kluwer-Academic, London, **226**, 361 (1992).
- [4] Chi-hung Huang, L. Mc Caughan, D. M. Gill, J. Light. Technol. **12**, 803 (1994).
- [5] N. N. Puscas, D. M. Grobnic, I. M. Popescu, M. Guidi, D. Scarano, G. Perrone, I. Montrosset, Optical Engineering **35**(5), 1311 (1996).
- [6] E. Desurvire. Erbium-Doped Fiber Amplifiers, J. Wiley & Sons, Inc. New York, 1994.
- [7] D. E. McCumber. Theory of phonon-terminated Masers, Phys. Rev. **134**, 299 (1964).
- [8] N. N. Puscas, B. Wacogne, V. Voinot, R. Ferrière. SPIE, **4430**, 398 (2001).
- [9] N. N. Puscas, A. Ducariu, G. C. Constantin, D. Dinu, J. Optoelectron. Adv. Mater. **7**(2) 1057 (2005).

*Corresponding author: pnt@physics.pub.ro